



A comprehensive assessment of MPPT algorithms to optimal power extraction of a PV panel

Claude Bertin Nzoundja Fapi^{a, b, *}, Martin Kamta^a, Patrice Wira^b

^aLESIA Laboratory, University of Ngaoundere, P.O. Box: 455 Ngaoundere, Cameroon

^bIRIMAS Laboratory, University of Haute Alsace, 61 Rue Albert Camus, 68200 Mulhouse, France

*Email: nzoufaclaubert@yahoo.fr

ARTICLE INFO

Received: 12 Aug 2019
Received in revised form:
17 Sept 2019
Accepted: 14 Sept 2019
Available online: 28 Oct
2019

Keywords:

Photovoltaic panel,
Maximum Power Point
Tracking, weather
conditions, MPPT
algorithms.

ABSTRACT

The electrical energy produced by photovoltaic (PV) process is inexhaustible, developable everywhere and clean. Whatever the conditions, it is desirable to extract the biggest amount of power from the solar panel. This is achieved with the use of a Maximum Power Point Tracking (MPPT) algorithm. Fluctuations in weather conditions (irradiation and temperature) strongly degrade the performance of the photovoltaic module's energy conversion and therefore all the power cannot be transferred to the load. The objective is to study and compare different approaches of MPPT algorithms to evaluate the power extracted under the standard test conditions and varying weather conditions. Results of the performance with all these algorithms are compared under different operating conditions. The results show that the Fuzzy Logic Controller (FLC) is the fastest in terms of stabilization and is followed respectively by Fractional Short-Circuit Current (FSCC), Fractional Open-Circuit Voltage (FOCV), Perturb and Observe (P&O), Incremental Conductance (INC) and Hill Climbing (HC) algorithms. The FLC also gives the best results in extracting, followed by P&O, INC, HC, FSCC and FOCV algorithms.

© 2019 Published by University of Tehran Press. All rights reserved.

1. Introduction

Over the past few years, the demand for electrical energy has never ceased as the constraints associated with its production have increased [1, 2]. Indeed, more and more power will be produced by the photovoltaic process which converts of sunlight into electricity. The drawbacks of this source of energy are the intermittence of the photovoltaic source and the fact that power supplied by the photovoltaic generator depends on unpredictable weather conditions. In order to overcome them, the implementation of a Maximum Power Point Tracking (MPPT) strategy to extract at any time the maximum power is another way to optimize the energy production. Indeed, the improvement of the efficiency of the photovoltaic generator requires optimal operation of the DC-DC converters used as an interface between the photovoltaic generator and the load to be supplied [3-11].

To ensure that the photovoltaic system will operate at its highest efficiency, many MPPT algorithms have

been developed. For example: Fractional Open-Circuit Voltage (FOCV) Algorithm [12-13], Fractional Short-Circuit Current (FSCC) Algorithm [12-14], Hill Climbing (HC) [5-9], Perturb & Observe (P&O) Algorithm [12-15], Incremental Conductance (INC) Algorithm [14-16], Bisection Numerical Algorithm (BNA), [15, 16], Artificial Neural Network (ANN) technique and the Fuzzy Logic Control (FLC) [17-20].

A photovoltaic system mainly consists of a PV panel, a DC-DC adaptation stage with an MPPT algorithm and a load as represented by Figure 1. Indeed, the design of a DC-DC adaptation stage corresponds to the modeling of the basic functions of a DC-DC converter. The latter is achieved by the notion of conservation of the power transferred by a static converter [21-25]. This power conversion corresponds to the relations between the four electrical quantities on the input and output points which are its currents and its voltages. The role of the DC-DC converter is to achieve an adaptation between the PV panel and the DC load to

have a maximum power transfer [26-27]. The operating point is therefore maintained in the vicinity of the Maximum Power Point (MPP) according to the operating conditions. The objective is to study and compare six different approaches of MPPT algorithms to evaluate the power extracted under the standard test conditions and varying weather conditions.

In this article, a new FLC method is developed. The design proposed addresses two key questions. First of all, although conventional MPPT are appropriate methods for a PV system under a slow change of irradiation, they face substantial challenges under a quick change. The

secondary problem is that the difficult engineering problems of a fuzzy system are reduced when there are few functions designed for members. The fuzzy rules of the proposed method are obtained from a modified conventional MPPT algorithm. The proposed technique allows the maximum power point to be accurately monitored and the drift problem to be avoided. After introduction modeling of the PV system is presented in Section 2. Then in Section 3, an MPPT methodology is analyzed. The results of the simulations and conclusion of the work are given respectively in Section 4 and Section 5.

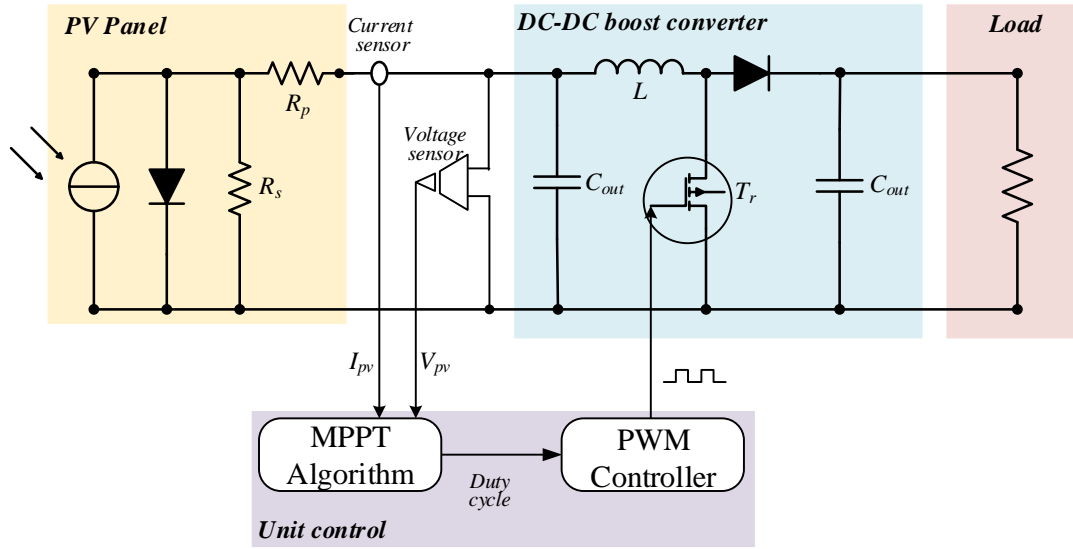


Figure 1. Electrical synoptic of the PV system.

2. PV Model and Characteristics

A PV cell is an electronic component that, when exposed to light (photons), produces electricity thanks to the photovoltaic effect. The circuit consists of two resistors and a diode is shown in Figure 2 [18, 24]. R_p indicates the presence of a leakage current in the P-N junction while R_s reports the resistivity of the material and the semiconductor-metal contact, the diode represents the electron-hole recombination in the P-N junction.

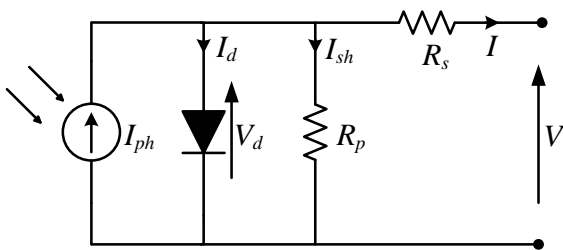


Figure 2. Model with a single diode of a PV cell.

By applying Kirchhoff's laws on the circuit of Figure 2 above, the cell generated current is given by [18, 24]:

$$I = I_{ph} - I_o \left[\exp \left(\frac{V + R_s I}{n N_{sc} V_T} \right) - 1 \right] - \frac{V + R_s I}{R_p} \quad (1)$$

where V and I are respectively voltage and current, I_o is the diode reverse saturation current, I_{ph} is the generated photocurrent, V_T is the thermal voltage ($V_T = kT / q$), k is the Boltzmann constant, n is the diode ideality factor, q is the electron charge and T is the cell's temperature (Kelvin).

The parameters of the Solkar36w PV panel used in this paper under the Standard Test Condition (STC: 25 °C and 1 kW/m²) are listed in Table I [24].

Table I. Solkar36w PV panel parameters.

Parameters	Symbols	Values
Maximum power	P_{mpp} (W)	40
Maximum voltage	V_{mpp} (V)	16.56
Maximum current	I_{mpp} (A)	2.25
Open-circuit voltage	V_{oc} (V)	21.24
Short-circuit current	I_{sc} (A)	2.55
Voltage coefficient	K_v (V/K)	-1.0017
Current coefficient	K_i (A/K)	0.032
Total Number of series cells	N_{sc}	36

In the Maximum Power Point (MPP) determination of the Solkar36w panel, the most important step is to determine the current - voltage and power - voltage characteristics. Figure 3 shows the I-V and P-V characteristic curves under the STC [24].

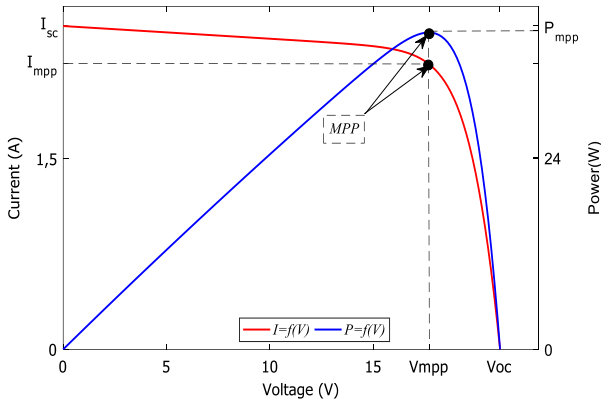


Figure 3. P-V and I-V characteristic of the Solkar36w PV panel.

3. MPPT Algorithms

The main aim of these MPPT commands is to find the MPP by keeping a good fit between the MPP and the load to ensure the transfer of maximum available electrical power.

3.1. Focv: Fractional Open-Circuit Voltage

The technique is simple and easy to implement. The method process flow chart is described by Figure 4. The Fractional Open-Circuit Voltage (FOCV) algorithm is based on a linear relationship between the open circuit voltage and the voltage at the peak power point [1, 4, 7]. Its expression is as follows:

$$V_{mpp} = K_v \times V_{oc} \tag{2}$$

where K_v is the voltage proportionality constant.

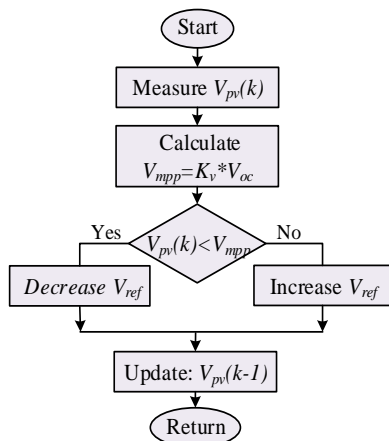


Figure 4. The FOCV technique flowchart.

3.2. FSCC: Fractional Short-Circuit Current

The method process flow chart is described by Figure 5. The Fractional Short-Circuit Current (FSCC)

algorithm is a technique based on the linear relationship between the short-circuit current and the current at the point of maximum power [1, 4, 7]. Its expression is as follows:

$$I_{mpp} = K_i \times I_{sc} \tag{3}$$

where K_i is the constant of proportionality.

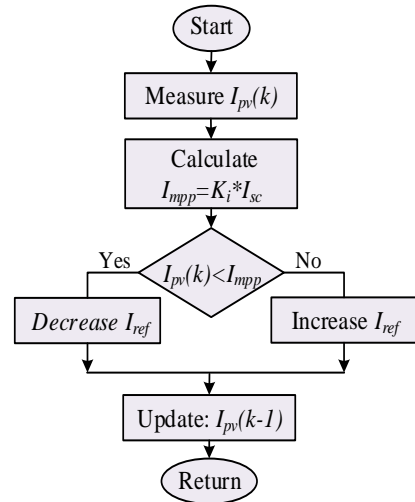


Figure 5. The FSCC algorithm flowchart.

3.3. Hc: Hill Climbing

The Hill Climbing (HC) algorithm calculates the duty cycle in each sampling period by comparing the current power to the previous one [1-3, 7]. The flow diagram of the HC algorithm is shown in Figure 6 [11]. The duty cycle in every sampling period is given by the comparison of the power at actual time and prior time. If the incremental power $dP > 0$, the duty cycle should be increased in order to make $dD > 0$. If $dP < 0$, the duty cycle is then reduced to make $dD < 0$.

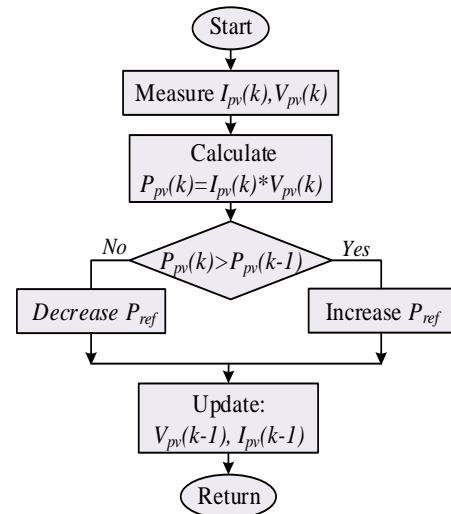


Figure 6. Flowchart of HC technique.

3.4. P&O: Perturb and observe

The Perturb and Observe (P&O) algorithm is based on a periodic disturbance of the voltage at the

photovoltaic module's output and by comparison of this disturbed output power with that of the previous disturbance cycle [1-5]. Figure 7 illustrates the flowchart of the P&O MPPT command [6-8]. To determine the power at each moment, two sensors are needed to measure the values of voltage and current. For a disturbance of the voltage, if the power decreases, the direction of the disturbance is maintained. If not, it is inverted so that the operating point converges towards the MPP.

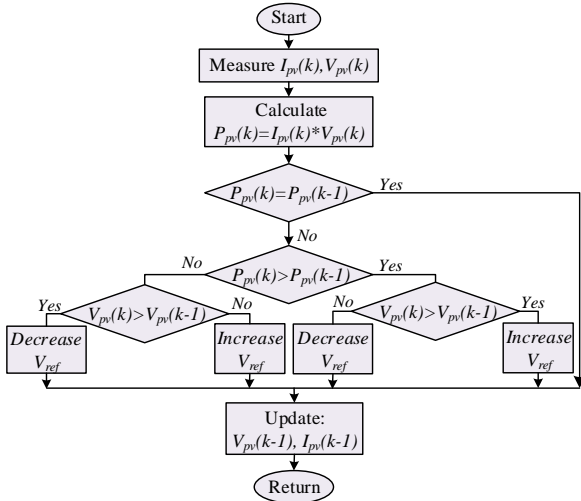


Figure 7. Flowchart of the P&O method.

3.5. Inc: Incremental of conductance

The Incremental of Conductance (INC) algorithm uses the conductance value and the increment of the conductance to deduce the position of the next operating point as close as possible to the point of maximum power [3-7]. The method process flow chart is described by Figure 8 [11].

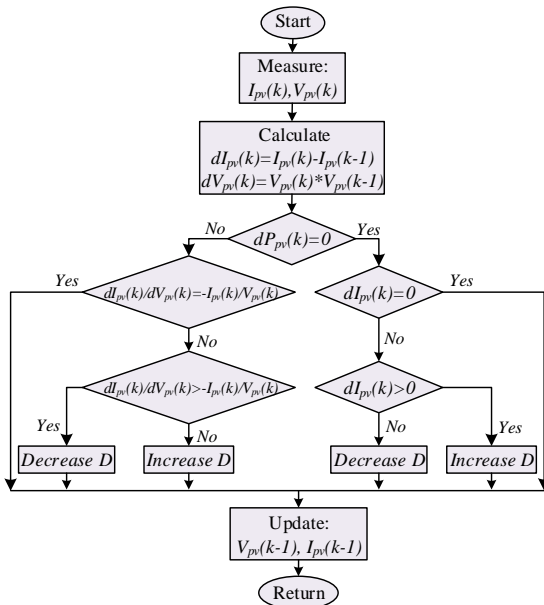


Figure 8. Flowchart of the INC algorithm.

3.6. FLC: Proposed Fuzzy logic control

The Fuzzy Logic Control (FLC) algorithm works with inaccurate inputs that do not require a precise mathematical model [1, 2, 4]. The error E and error change CE at times samples k are the two FLC inputs [18-20]. Its output is a PWM signal that controls the boost converter. The two input variables are given by:

$$E(k) = \frac{\Delta P}{\Delta I} = \frac{P(k) - P(k-1)}{I(k) - I(k-1)} \quad (4)$$

$$dE(k) = E(k) - E(k-1) \quad (5)$$

where $P(k)$ and $I(k)$ are respectively the power and the current of the PV panel, $E(k)$ indicates if the point of operation of the load at the moment k is located to the left or right of the MPP on the power characteristic curve of Figure 3. $dE(k)$ shows the direction of shifting of this point. The FLC contains Fuzzification, basic rule and defuzzification.

Fuzzification consists of converting the digital inputs into linguistic variables based on the degree of member functions. Figure 9 illustrates the fuzzy sets: (a) the input error, (b) the input of the error change and (c) the output that contains seven triangular membership functions.

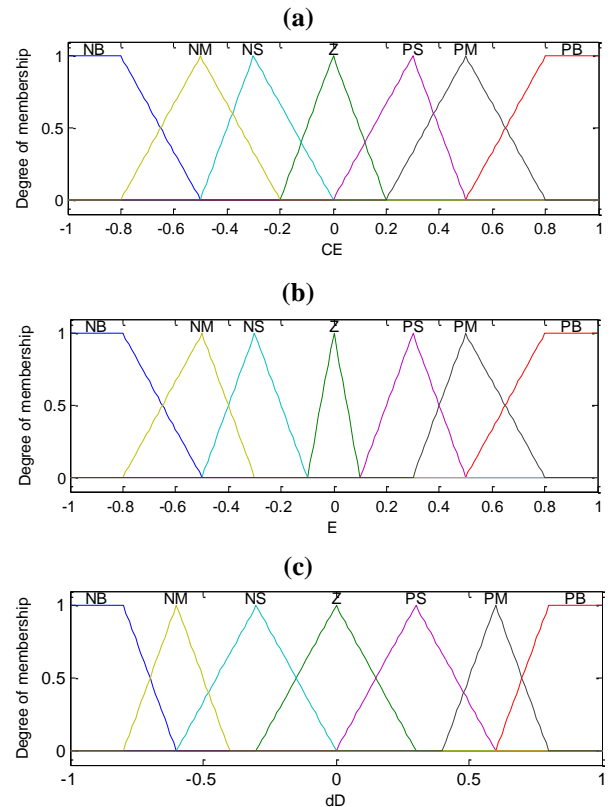


Figure 9. Membership functions, (a) for $E(k)$, (b) for $dE(k)$, and (c) for D .

The rules between the inputs and the output have to be established. Table II shows the fuzzy controller rule table where all the matrix inputs are the fuzzy sets of

$E(k)$, $dE(k)$, and D . Here is an example of a control rule from Table II:

if E is NL and dE is NW then D is NM

Table II. Rules of the Fuzzy System.

		dE						
		NF	NW	NW	Z	PL	PW	PF
E	NF	NF	NF	NF	NW	NW	NL	Z
	NW	NF	NF	NW	NW	NL	Z	PL
	NL	NF	NM	NM	NL	Z	PL	PW
	Z	NM	NM	NL	Z	PL	PW	PW
	PL	NM	NL	Z	PL	PW	PW	PF
	PW	NL	Z	PL	PW	PM	PF	PF
	PF	Z	PL	PW	PW	PF	PF	PF

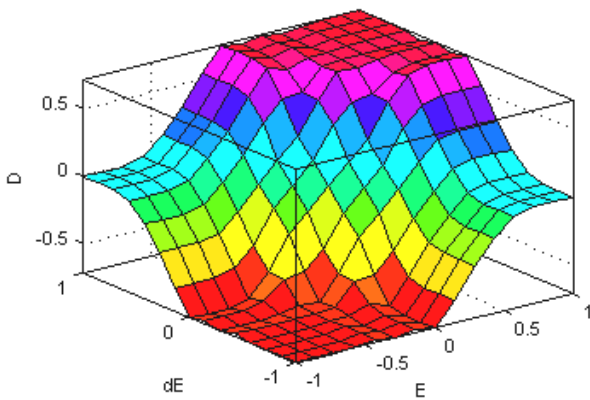


Figure 10. Three-dimensional surface corresponding to the membership in Figure 9 and the rule in Table II.

Defuzzification consists of converting the output of the linguistic variable into a precise numeric variable (D):

$$D = \frac{\sum_{j=1}^n \mu(D_j) - D_j}{\sum_{j=1}^n \mu(D_j)} \quad (6)$$

4. Results and Discussion

In this section, the standalone PV system in Figure 1, which consists of a solar panel, a DC-DC boost converter with its MPPT command and load is implemented and simulated in the MatLab/Simulink environment. The Solkar36w is the photovoltaic module used for our study. The latter produces a power of 40 W in the STC (see Table 1). In order to transfer all this power to the load, the Boost converter used receives simultaneously the current and voltage from the PV panel and a control signal from the MPPT controller with a switching frequency of 10 KHz.

In this paper, the value of the boost inductance is 290 μ H, the capacitors of the input and output filters are 250 μ F and 330 μ F respectively. The switching frequency used is 10 kHz and a resistance load of 250 Ω .

In order to validate the effectiveness of the different MPPT methods, the latter are tested using respectively, the Standard test conditions and the Changes of the solar irradiance with a constant temperature of 25 °C cases. The results of the power of the PV of algorithms are shown in Figure 11 and Figure 12.

4.1. Case 1: Standard test conditions

In this case, the six algorithms are evaluated for $G = 1000 \text{ W/m}^2$ and $T = 25 \text{ }^\circ\text{C}$. Figure 11 shows the power extracted from the PV panel and delivered to the load with the six methods in a simulation test over duration of 0.5 s. By analyzing the power curves produced by the PV module using the different MPPT algorithms in Figure 11. Two points have been enlarged; it appears from its bridges that the response times are 5 ms for FLC, 60 ms for P&O algorithm, 70 ms for the INC algorithm, 150 ms for the HC algorithm, 20 and 20 ms respectively for the FSCC and FOCV algorithms.

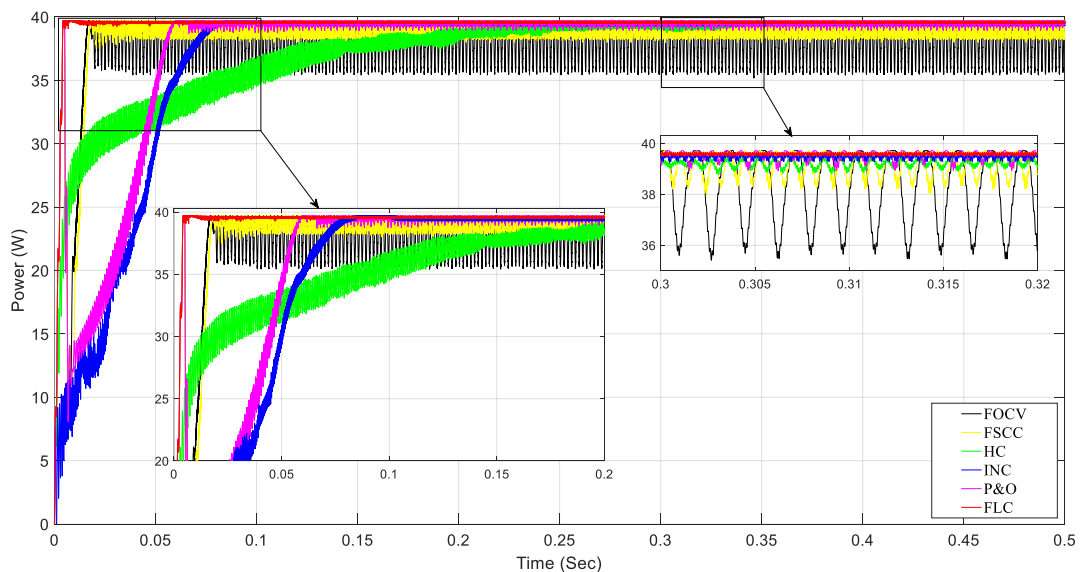


Figure 11. The output power of PV system with the 6 MPPT methods.

4.2. Case 2: Changes of the solar irradiance with a constant temperature of 25 °C

Figure 12 shows a test for varying weather conditions. Initially, $G = 1000 \text{ W/m}^2$, goes to 800 W/m^2 , rises to 900 W/m^2 then decreases to 750 W/m^2 and finally reaches 950 W/m^2 . Changes in irradiance were made every 0.2 s with total simulation duration of 1 s. It can be

observed that the FLC algorithm gives the best results by extracting 39.65 W, followed by the P&O algorithms (39.5 W), INC (39.4 W), HC (38.5 W), FSCC (37.5 W) and FOCV (37 W). In addition, the proposed FLC converges to the MPP with a fast response time, higher performance and a small static error compared to other algorithms during irradiation changes.

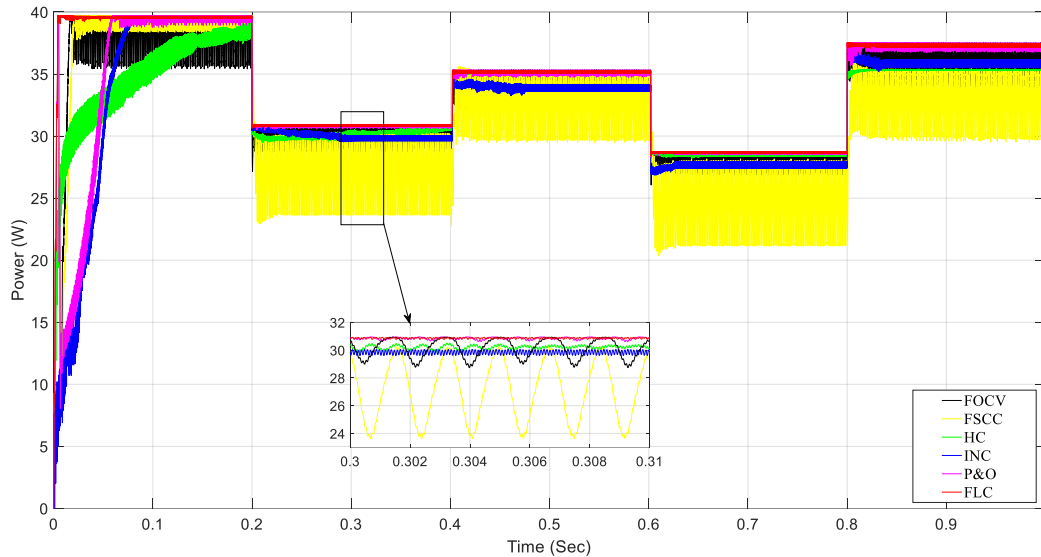


Figure 12. The performance of the different MPPT algorithms.

4.3. Performance of MPPT algorithms

Results with all these algorithms are compared under different operating conditions. The tracking efficiency (η) is an important parameter in the MPPT algorithm [2, 4, 6]. This value is calculated as follows:

$$\eta = \frac{\int_0^t P_{mppt}(t)dt}{\int_0^t P_{max}(t)dt} \times 100 \quad (7)$$

A summary of the performance indicators of the 6 algorithms is presented in Table III. The FLC is the fastest in terms of stabilization and is followed respectively by FSCC, FOCV, P&O, INC and HC algorithms. The FLC also gives the best results in extracting, followed by P&O, INC, HC, FSCC and FOCV algorithms.

Table III. Comparison of different MPPT algorithms.

Temperature, Irradiation	Parameters	Algorithms					
		FLC	P&O	INC	HC	FSCC	FOCV
T=25°C G=1000W/m²	Maximum power from the PV (W)	40	40	40	40	40	40
	PV output power (W)	39.65	39.5	39.4	38.5	37.5	37
	Tracking efficiency (%)	99,10	98,75	98,50	96,25	93,75	92,50
	Ripple rate (%)	0.25	1.02	1.02	1.27	5.26	10.81
	Response time (s)	0.005	0.06	0.07	0.15	0.02	0.02
	Implementation complexity	Complex	Medium	Medium	Simple	Simple	Simple
	Initial sitting parameters	3	2	2	2	1	1
	The uses sensors	Voltage Current	Voltage Current	Voltage Current	Voltage Current	Current	Voltage

5. Conclusion

Results with all these algorithms are compared under different operating conditions and shows that the FLC algorithm is the fastest in terms of stabilization time with a response time of 5 ms. This approach also presents

very low oscillations around the operating point. The response times are 60 ms for P&O algorithm, 70 ms for the INC algorithm, 150 ms for the HC algorithm, 20 and 20 ms respectively for the FSCC and FOCV algorithms. The power generated with the different MPPT algorithms is evaluated at the maximum power point with a 40 W

photovoltaic module. The FLC algorithm gives the best results by extracting 39.65 W, followed by the P&O algorithms (39.5 W), INC (39.4 W), HC (38.5 W), FSCC (37.5 W) and FOCV (37 W).

Acknowledgement

The authors acknowledge the contribution of the **Pierre-et-Jeanne Spiegel Foundation** for its financial support.

References

1. Rezk, H. and A. M. Eltamaly, *A comprehensive comparison of different MPPT techniques for photovoltaic systems*. Solar Energy, 2014. **112**: p. 1-11.
2. Nzoundja, Fapi, C. B., P. Wira, M. Kamta, A. Badji, and H. Tchakounte, *Real-time experimental assessment of Hill Climbing MPPT algorithm enhanced by estimating a duty cycle for PV system*. International Journal of Renewable Energy Research (IJRER), 2019. **9**(3): p. 1180-1189.
3. Tofoli, F. L., D. de C. Pereira, and W. J. de Paula, *Comparative Study of Maximum Power Point Tracking Techniques for Photovoltaic Systems*. International Journal of Photoenergy - Hindawi, 2015. **2015**: p. 1-10.
4. Danandeh, M. A. and S. M. Mousavi, *Comparative and comprehensive review of MPPT methods for PV cells*. Renewable and Sustainable Energy Reviews, 2018. **82**: p. 2743-2767.
5. Dadjé, A., N. Djongyang, J. D. Kana, and R. Tchinda, *Maximum power point tracking methods for photovoltaic systems operating under partially shaded or rapidly variable insolation conditions: a review paper*. International Journal of Sustainable Engineering, 2016. **9**(4): p. 224-239.
6. Subudhi, B. and R. R. Pradhan, *A comparative study on maximum power point tracking techniques for photovoltaic power systems*. IEEE Transactions Sustainable Energy, 2013. **4**(1): p. 89-97.
7. Boukenoui, R., R. Bradai, A. Mellit, M. Ghanes, and H. Salhi, *Comparative Analysis of P&O, Modified Hill Climbing-FLC, and Adaptive P&O-FLC MPPTs for Microgrid Standalone PV System*. in 4th International Conference on Renewable Energy Research and Applications (ICRERA), Palermo, Italy, 22-25 Nov 2015. p. 1095-1099.
8. Mazaheri, S. P. and D. Solyali, *A review on maximum power point tracker methods and their applications*. Journal of Solar Energy Research (JSER), 2018. **3**(2): p. 123-133.
9. Nzoundja, Fapi, C. B., A. Badji, H. Tchakounte, G. Tsayo, Bantio, M. Kamta, and P. Wira, *Assessment of two MPPT algorithms for a standalone photovoltaic system with variable weather condition*. International Journal of Engineering & Technology (UAE), 2018. **7**(4): p. 6790-6796.
10. Belkaid, A., I. Colak, and K. Kayisli, *A Comprehensive study of different photovoltaic peak power tracking methods*. in 6th International Conference on Renewable Energy Research and Applications (ICRERA), San Diego, USA, 5-8 Nov. 2017. p. 1073-1079.
11. Razzazan, M., Z., Mirbagheri, and A. Ramezani, *Maximum Power Point Tracking Using Constrained Model Predictive Control for Photovoltaic Systems*. Journal of Solar Energy Research (JSER), Spring (2017). **2**(2): p. 19-24.
12. Mohapatra, A., B. Nayak, P. Das, and K. B. Mohanty, *A review on MPPT techniques of PV system under partial shading condition*. Renewable and Sustainable Energy Reviews, 2017. **80**: p. 854-867.
13. Esram, T. and P. L. Chapman, *Comparison of photovoltaic array maximum power point tracking techniques*. IEEE Transactions on Energy Conversion, 2007. **22**(2): p. 439-449.
14. Saravanan, S. and N. R. Babu, *Maximum power point tracking algorithms for photovoltaic system - A review*. Renewable and Sustainable Energy Reviews, 2016. **57**: p. 192-204.
15. Bayat, P. and A. Baghrmian, *A High Efficiency On-board Charger for Solar Powered Electric Vehicles Using a Novel Dual-output DC-DC Converter*. Journal of Solar Energy Research (JSER), Spring (2019). **4**(2): p. 128-141.
16. Belkaid, A., I. Colak, and K. Kayisli, *Implementation of a modified P&O-MPPT algorithm adapted for varying solar radiation conditions*. Electrical Engineering - Springer, 2017. **99**(3): p. 839-846.
17. Nafeh, A. E.-S. A., F. H. Fahmy, and E. M. Abou, El-Zahab, *Evaluation of a proper controller performance for maximum power point tracking of a standalone PV system*. Solar Energy Materials and Solar Cells, 2003. **75**(3): p. 723-728.
18. Batzelis, I. E., *Simple PV performance equations theoretically well founded on the single-diode model*. IEEE Journal of Photovoltaics, 2017. **7**(5): p. 1400-1409.
19. Rodrigues, E. M. G., R. Godina, M. Marzband, and E. Pouresmaeil, *Simulation and Comparison of Mathematical Models of PV Cells with Growing Levels of Complexity*. Energies (MDPI), 2018. **11**(2902): p. 2-21.
20. Gang, M., X. Guchao, C. Yixi, and J. Rong, *Voltage stability control method of electric springs based on adaptive PI controller*. Electrical Power and Energy Systems, 2018. **95**: p. 202-212.
21. Yilmaz, U., A. Kircay, and S. Borekci, *PV system fuzzy logic MPPT method and PI control as a charge controller*. Renewable and Sustainable Energy Reviews, 2018. **81**: pp. 994-1001.
22. Tang, S., Y. Sun, and Y. Chen, *An enhanced MPPT method combining fractional-order and fuzzy logic*

- control*. IEEE Journal of Photovoltaics, 2017. **7**(2): p. 640-650.
23. Suganthi, L., S. Iniyan, Anand, and A. Samuel, *Applications of fuzzy logic in renewable energy systems – A review*. Renewable and Sustainable Energy Reviews, 2015. **48**: p. 585-607.
 24. Nzoundja, Fapi, C. B., P. Wira, and M. Kamta, *A Fuzzy Logic MPPT Algorithm with a PI Controller for a Standalone PV System under Variable Weather and Load Conditions*. in IEEE International Conference on Applied Smart Systems (ICASS), Medea, Algeria, 24-25 Nov. 2018. p. 1-6.
 25. Mehdipour, C. and F. Mohammadi, *Design and Analysis of a Stand-Alone Photovoltaic System for Footbridge Lighting*. Journal of Solar Energy Research (JSER), Spring (2019). **4**(2): p. 85-91.
 26. Karami, N., N. Moubayed, and R. Outbib, *General Review and classification of different MPPT Techniques*. Renewable and Sustainable Energy Reviews, 2017. **68**: p. 1-18.
 27. Enrique, J. M., E. Durán, M. Sidrach-de-Cardona, and J. M. Andújar, *Theoretical assessment of the maximum power point tracking efficiency of photovoltaic facilities with different converter topologies*. Solar Energy, 2007. **81**(1): p. 31-38.